



## Quantitative clay mineralogy predicts radiocesium bioavailability to ryegrass grown on reconstituted soils



Margot Vanheukelom <sup>a,b,\*</sup>, Lieve Sweeck <sup>a</sup>, May Van Hees <sup>a</sup>, Nancy Weyns <sup>d</sup>, Jos Van Orshoven <sup>c</sup>, Erik Smolders <sup>b</sup>

<sup>a</sup> Biosphere Impact Studies, Belgian Nuclear Research Centre (SCK CEN), Boeretang 200, 2400 Mol, Belgium

<sup>b</sup> Division of Soil and Water Management, KU Leuven, Kasteelpark Arenberg 20, 3001 Leuven, Belgium

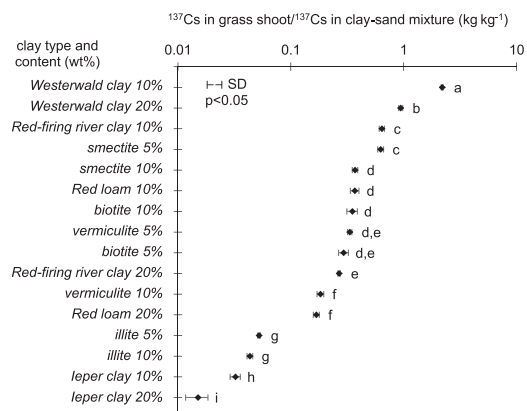
<sup>c</sup> Division of Forest, Nature and Landscape, KU Leuven, Celestijnenlaan 200e - box 2411, 3001 Leuven, Belgium

<sup>d</sup> Division of Geology, KU Leuven, Celestijnenlaan 200e - box 2411, 3001 Leuven, Belgium

### HIGHLIGHTS

- Clay mineralogy and clay content in substrates affect  $^{137}\text{Cs}$  uptake in grass.
- XRD detected fractions of clay minerals can predict  $^{137}\text{Cs}$  soil-plant transfer.
- Soil exchangeable K and radiocesium sorption explain  $^{137}\text{Cs}$  soil-plant transfer.

### GRAPHICAL ABSTRACT



### ARTICLE INFO

Dataset link: [Vanheukelom2022\\_XRD-pattern \(Original data\)](#) Editor: Filip M.G. Tack

#### Keywords:

Mineral composition  
X-ray diffraction  
Radiocesium interception potential  
Pot cultivation experiment  
Grass  
 $^{137}\text{Cs}$  transfer factor

### ABSTRACT

Current radiocesium ( $^{137}\text{Cs}$ ) models to evaluate the risk of  $^{137}\text{Cs}$  transfer from soil to plants are based on the clay and exchangeable potassium (K) contents in soil. These models disregard the mineralogy of the clay fraction and are likely not capable of accurately predicting the  $^{137}\text{Cs}$  transfer factor (TF) in soils of contrasting parent rocks and weathering stages. The objectives of this study were to test that hypothesis and to identify whether quantitative information on mineralogy can improve the predictions. A pot cultivation experiment was set up with clay-sand mixtures in single and double clay doses that were fertilized, spiked with  $^{137}\text{Cs}$  and grown with ryegrass for 30 days. Four clays (illite, biotite, smectite and vermiculite) along with six deposits from clay-rich geological units were compared. The TF generally decreased with increasing clay dose for each of these ten different clay groups, however, the TF varied two orders of magnitude across clay groups and doses. The TF was highest for clays with little  $^{137}\text{Cs}$  specific sites such as bentonite and/or where the exchangeable K content was low compared to the other clays. The TF was well predicted from the soil solution  $^{137}\text{Cs}$  and K concentrations ( $R^2 = 0.72$  for log transformed TF), corroborating earlier findings in natural soils. The TF (log transformed) was statistically unrelated to total phyllosilicate content or 1:1 and 2:1:1 type phyllosilicate content while it significantly decreased with increasing 2:1 phyllosilicate content ( $R^2 = 0.32$ ). A multiple regression model with four different X-ray diffraction (XRD) based phyllosilicate groups yielded the strongest predictive power ( $R^2 = 0.74$ ). We conclude that XRD quantification is valuable for describing  $^{137}\text{Cs}$  bioavailability in plant substrates. These findings now await confirmation for natural soils.

\* Corresponding author at: Biosphere Impact Studies, Belgian Nuclear Research Centre (SCK CEN), Boeretang 200, 2400 Mol, Belgium.

E-mail addresses: [margot.vanheukelom@sckcen.be](mailto:margot.vanheukelom@sckcen.be) (M. Vanheukelom), [lieve.sweeck@sckcen.be](mailto:lieve.sweeck@sckcen.be) (L. Sweeck), [erik.smolders@kuleuven.be](mailto:erik.smolders@kuleuven.be) (E. Smolders).

## 1. Introduction

After nuclear incidents, radiocesium (e.g.  $^{137}\text{Cs}$ ) can be released into the environment. Fallout radiocesium is deposited mainly in ionic form, attached to aerosols, in large-scale incidents (Bunzl et al., 1995). When deposited on agricultural land, it can enter the food chain, which poses a risk to human health (International Atomic Energy Agency, 2009). To manage this risk, decision-makers need models to predict the extent of transfer of  $^{137}\text{Cs}$  from soil to plants. Plant roots absorb the  $^{137}\text{Cs}$  from the soil solution and its concentration depends on the total amount deposited and on the sorption to soil particles. It is generally known that the adsorption of  $^{137}\text{Cs}$  cations at trace concentrations is controlled by the sorption on the highly selective Frayed Edge Sites (FES) of phyllosilicates (Sawhney, 1972). The FES constitute the wedge-shaped zones between closed and open interlayers of weathered mica-like minerals where the  $^{137}\text{Cs}$  cations are very selectively sorbed. The FES content of phyllosilicates varies largely, ranging between high for weathered micas such as illite to vanishingly low for kaolinite, unweathered micas and some smectites (Durrant et al., 2018; Missana et al., 2014). Not all minerals have these FES to the same extent, so the selective adsorption of  $^{137}\text{Cs}$  cations in soils is determined by the type and content of minerals. The mineralogy of the soil is governed by the parent material and the weathering stage and, hence, it is predictable that  $^{137}\text{Cs}$  bioavailability is also affected by soil weathering stage and its content of phyllosilicates.

The bioavailability of  $^{137}\text{Cs}$  not only depends on the FES content but also on the prevailing concentration of competing ions of which potassium (K) and ammonium ( $\text{NH}_4^+$ ) cations are most relevant. The  $\text{NH}_4^+$  concentration in soils is less important under the aerobic conditions needed for most food crops in temperate regions. The bioavailability of  $^{137}\text{Cs}$  is a complex function of the K concentration in solution. On the one hand, K and  $^{137}\text{Cs}$  cations compete for non-selective adsorption on soil particles; on the other hand, K and  $^{137}\text{Cs}$  cations compete for uptake through plant roots (Shaw and Bell, 1991). Of particular interest is the latter where the concentration of K controls how much  $^{137}\text{Cs}$  can be transferred from solution to the plant. At K concentrations in soil solution of the order of  $<1 \text{ mmol L}^{-1}$ , the plant uptake of  $^{137}\text{Cs}$  from solution sharply increases with decreasing K concentrations (Smolders et al., 1997). If the K concentration is higher, the  $^{137}\text{Cs}$  uptake from solution is almost unaffected by the K concentration.

The bioavailability of  $^{137}\text{Cs}$ , generally defined as the ability of  $^{137}\text{Cs}$  to move from the soil to the plant compartment in the environment (Desmet et al., 1991; Semple et al., 2004), is expressed by the  $^{137}\text{Cs}$  soil-to-plant transfer factor (TF), which is the ratio of the  $^{137}\text{Cs}$  concentration in the plant material to that in the soil (International Atomic Energy Agency, 2009). The retention of  $^{137}\text{Cs}$  on the FES in the soil can be quantified as the Radiocesium Interception Potential (RIP) (Cremers et al., 1988). The RIP is defined as the product of the selectivity coefficient of Cs to K and the FES capacity of the soil particles assuming that K is the only cation which saturates the FES. The RIP of a soil can be determined experimentally by the method proposed by Wauters et al. (1996a, 1996b, 1996c) and the solid-liquid distribution coefficient  $K_D$  of  $^{137}\text{Cs}$  is the RIP divided by the concentration of the competing cations in solution. In the plant compartment, the uptake of  $^{137}\text{Cs}$  is controlled by the soil solution  $^{137}\text{Cs}$  and K concentrations. Taken together, it follows that the TF depends on the RIP of the soil and the soil solution K concentration; both these variables depend in turn on the clay content, the mineralogy, and the exchangeable K content. The  $^{137}\text{Cs}$  TF has been experimentally determined for many soil and plant type combinations (International Atomic Energy Agency, 2010). Models created based on the concepts described above predict the TF based on the clay-size particle content and the exchangeable K content, thereby assuming one mean value for the RIP per unit clay (Absalom et al., 1999, 2001; Tarsitano et al., 2011). Current  $^{137}\text{Cs}$  transfer models fail to predict the TF for a set of distinct soil types (Almahayni et al., 2019; Uematsu et al., 2016). A possible explanation is that the clay mineralogy is ignored and the RIP per unit of clay content in the soil may differ largely among soils at widely varying weathering stages. Only for soils formed from

similar parent rock or similar weathering stage as the soils used to develop the TF models (e.g. Sanchez et al., 1999; Smolders et al., 1997), the model predictions agree with the observations. Hence, it is expected that prediction of TF fails when soils with more contrasting parent materials and weathering stages are included. It can be speculated that quantitative mineralogy can improve the clay to RIP conversion and, hence, improve the TF prediction.

Against this background, this study was set up to identify whether quantitative mineralogy can improve the  $^{137}\text{Cs}$  TF prediction compared to predictions of existing TF models for  $^{137}\text{Cs}$  (Absalom et al., 1999, 2001; Tarsitano et al., 2011). As a first step, a greenhouse study was set up with reconstituted soils, i.e. clay-sand mixtures in single and double clay doses that were fertilized, spiked with  $^{137}\text{Cs}$  and grown with ryegrass for 30 days. We selected clays with contrasting properties and measured the RIP and TF of  $^{137}\text{Cs}$  in these model soils. We quantified the mineralogy of the clays using X-ray diffraction (XRD). Finally, we compared the experimentally observed  $^{137}\text{Cs}$  TF with the TF predicted either from exchangeable K and clay content or from a model that included XRD data.

## 2. Materials and methods

The experimental design is a pot experiment with a full factorial combination of ten different clays or clay deposits, each dosed at two levels in sand with three replicates.

### 2.1. Clay selection

Ten clays from subsurface geological units were collected (Table 1). Four commercially available mineral clays containing predominately 2:1 phyllosilicates were chosen: illite, biotite, smectite (bentonite) and vermiculite. Six clays were collected from deposits exploited by the ceramic industry consisting of various minerals: Boom clay, Campine clay, Ieper clay, Red-firing river clay, Red loam, and Westerwald clay. Both categories are noted here as 'clay'.

### 2.2. Clay composition and characterization

#### 2.2.1. Mineralogy

Subsamples were taken from the deposit clays to account for possible heterogeneities in composition among the multiple containers in which they were delivered. Only one subsample of the mineral clays was taken for analysis. The subsamples were oven-dried ( $60^\circ\text{C}$ ). They were crushed by pestle and mortar until all material passed through a 0.5 mm sieve. Each sample was prepared following the internal standard method for powder XRD (Šrodoň et al., 2001), with the addition of 10 wt% zincite ( $\text{ZnO}$ ) of known weight ( $\pm 0.001 \text{ g}$ ) for quantification purposes. The clay and  $\text{ZnO}$  were milled (McCrone Micronizing Mill) together with about 4 mL of ethanol for 5 min to obtain a homogenous mixture. The mixture was placed under a fume hood until dry. The mixture was passed through a 0.355 mm sieve to obtain a fine powder. Next, the powder was inserted in a side-loading holder by gently tapping the holder on a flat surface to distribute the powder evenly throughout the holder cavity. The XRD measurements were carried out with a diffractometer (PW1830, Philips) in a Bragg-Brentano arrangement and 173 mm goniometer radius. The diffractometer was equipped with  $\text{Cu-K}_{\alpha}$  radiation, a graphite crystal monochromator and a gas proportional detector. The powders were scanned at 45 kV and 30 mA and ranging over  $5\text{--}65^\circ 2\theta$  with  $0.02^\circ 2\theta$  step size and 2 s counting time. The minerals in the powder were identified and quantified using QUANTA (© Chevron ETC). The software uses the Mineral Intensity Factors method (Moore and Reynolds, 1997) where the sum of identified mineral phases is fitted to the recorded XRD pattern. The mineral identification procedure described by Moore and Reynolds (1997) was followed. The estimated quantities expressed as weight percentages (wt%) were normalized. The precision of the method was previously reported by Šrodoň et al. (2001) and the uncertainty was estimated to be 2–3 % per mineral phase.

**Table 1**

Selected properties of the studied mineral clays and deposit clays. The mineral composition, cation exchange capacity ( $CEC_{clay}$ ) and radiocesium interception potential ( $RIP_{clay}$ ). Mineral phases belonging to the same phyllosilicate structure group are summed up as 2:1 for micas and other 2:1 type phyllosilicates, 1:1 for kaolin and 2:1:1 for chloritic minerals. A more detailed mineral composition of the samples is given as supplementary material (Table A.1). Data is ordered by decreasing  $RIP_{clay}$  value. The standard deviations are given in brackets ( $n = 2$  or 3, see below).

Clay	Code	Origin	Mineral content					$CEC_{clay}$ <sup>a</sup> cmol <sub>c</sub> kg <sup>-1</sup>	$RIP_{clay}$ <sup>b</sup> mmol kg <sup>-1</sup>
			2:1 wt%	1:1	2:1:1	Quartz	Other		
Illite	ILL	Auvergne (France)	67.0	1.0	1.0	21.0	10.0	22.6 (0.2)	8400 (1460)
Ieper Group clay	IC	Rumbeke (Belgium)	55.1	6.3	2.9	22.5	13.2	30.8 (0.5)	5710 (170)
Boom Formation	BC	Rumst (Belgium)	45.3	10.0	2.0	28.8	13.5	19.2 (0.9)	5570 (100)
Red loam	RL	Veldwezelt (Belgium)	22.8	3.0	2.0	53.0	19.2	9.8 (0.5)	3480 (150)
Red-firing river clay	RFC	Hedikhuizen (The Netherlands)	25.4	3.7	2.7	58.5	9.7	9.3 (0.2)	3380 (200)
Campine Group clay	CC	Beerse (Belgium)	28.4	6.9	3.3	52.1	9.3	7.4 (0.1)	2560 (170)
biotite	BIO	Bancroft (Canada)	97.3	<0.1	<0.1	<0.1	2.7	2.9 (<0.1)	2430 (40)
Westerwald clay	WC	Boden (Germany)	15.6	18.0	<0.1	64.2	2.3	3.2 (0.1)	900 (15)
Vermiculite	VER	(Russia) <sup>c</sup>	86.0	<0.1	9.0	<0.1	5.0	106.5 (0.9)	523 (47)
Bentonite	BEN	Wyoming (USA)	92.6	<0.1	<0.1	3.0	4.4	71.7 (1.8)	385 (39)

<sup>a</sup>  $n = 2$ .

<sup>b</sup>  $n = 3$ .

<sup>c</sup> (Thiry, 1997; Thiry et al., 1996).

### 2.2.2. Selective and non-selective adsorption capacity

The radiocesium interception potential (RIP) and cation exchange capacity (CEC) were determined separately for the clays and sand for comparison with the clay-sand mixtures. The weight of air-dried samples was corrected for moisture content by oven-drying (105 °C) subsamples.

The RIP was determined based on the procedure described by Wauters et al. (1996a). The air-dry clays and sand were prepared in triplicate and brought into contact with a solution of 100 mmol L<sup>-1</sup> CaCl<sub>2</sub> and 0.5 mmol L<sup>-1</sup> KCl. The solid-liquid ratio (S:L) was 0.5 g clay or 2.0 g sand to 160 mL solution. The clays, a reference clay (illite du Puy, France) and sand were weighted in dry dialysis bags (VISKING®, MWCO 12–14 kDa) and filled with 10 mL of the Ca—K solution. The dialysis bags were transferred into bottles filled with 150 mL outer Ca—K solution for pre-equilibration and shaken end-over-end for 24 h. The outer solution was renewed and shaken again for 24 h. Finally, the outer solution was labelled with carrier-free <sup>137</sup>CsCl to obtain an activity of 200 kBq L<sup>-1</sup>. After 24 h of shaking, the outer solution was sampled and analyzed. The initial and remaining activity concentrations of <sup>137</sup>Cs in solution were measured using a NaI(Tl) gamma counter (1480 WIZARD 3", PerkinElmer). For every batch of four triplicates, at least four blanks were measured to correct for background counts. The adsorbed <sup>137</sup>Cs on the solid phase was calculated as the difference in solution <sup>137</sup>Cs between starting time and 24 h contact with the solid phase. The <sup>137</sup>Cs K<sub>D</sub> is calculated as the ratio of adsorbed <sup>137</sup>Cs (kBq kg<sup>-1</sup> soil) to that in solution (kBq L<sup>-1</sup>) and the RIP (mmol kg<sup>-1</sup>) is calculated as the ratio of K<sub>D</sub>, with the 0.5 mmol L<sup>-1</sup> K in solution. The RIP of the clay ( $RIP_{clay}$ ) and sand ( $RIP_{sand}$ ) were summed proportionally as they occur in the substrate ('RIP calculated'). A blank sample was also prepared following the same procedure but without clay or sand to determine the adsorption of <sup>137</sup>Cs on the membrane and in the bottle. The RIP of the blank was <0.1 mmol kg<sup>-1</sup>.

The CEC was determined following the cobalthexamine (cohex) method (Ciesielski and Sterckeman, 1997) with adjusted S:L depending on the CEC. The oven-dry (105 °C) clays and sand, prepared in duplicate, were brought into contact with 16.6 mmol L<sup>-1</sup> Co(NH<sub>3</sub>)<sub>6</sub>Cl<sub>3</sub> and placed in an end-over-end shaker for 1 h. After centrifugation, the supernatant was filtered at 0.45 μm (Acrodisc®). The initial and remaining Co concentrations in solution were measured using an inductively coupled plasma mass

spectrometer (7700 Series ICP-MS, Agilent Technologies). For the entire batch of duplicates, two blanks were measured twice to verify the quality of the measurement. The CEC was calculated as the difference of the Co equivalent charge concentration in solution per solid weight between samples before and after 1 h contact with the solid phase.

The CEC of the clay-sand mixtures ('CEC mixture') was determined before they were spiked (Section 2.3.1). The RIP of the clay-sand mixtures after plant growth ('RIP mixture') was determined by the method described above with 1 g of mixture.

### 2.3. Pot experiment

#### 2.3.1. Preparing clay-sand mixtures

Quartz sand was obtained from a building supply store (river sand, un-washed). The clays were mixed with sand to create the plant substrates. In these mixtures, however, clay particles were not fixed in a structure because these artificial substrates lacked aggregating agents such as organic matter and metal oxides, hence clay flocculation was required to limit the risk of clay migration during watering of plants. The illite, biotite, smectite and vermiculite were converted to the divalent form to enhance flocculation. The four clays were first ground and passed through a 1 mm sieve. The clays were bathed in a 0.4 mol L<sup>-1</sup> CaCl<sub>2</sub>, 0.1 mol L<sup>-1</sup> MgCl<sub>2</sub> and 0.025 mol L<sup>-1</sup> KCl solution with a S:L of 1 kg to 5 L. After 24 h, the clays were washed with deionized water and air-dried. The six deposit clays were left untreated because sufficient aggregating agents were present.

A single and double dose of clay was mixed with sand to study the effect of the dose of clay on <sup>137</sup>Cs transfer. The clay doses were 5 wt% or 10 wt% for the mineral clays and 10 wt% or 20 wt% for the deposit clays. The doses of the clay deposits were chosen larger because about half of the clay consisted of minerals that were not phyllosilicates (Table 1).

The clay-sand mixtures were fertilized and spiked with <sup>137</sup>Cs. A nutrient solution was composed, based on the hydroponic solution by Hoagland and Arnon (1950), so that it contained the elements necessary for plant and its growth would not be hampered by deficiencies. Importantly, the K concentration (2.84 mmol L<sup>-1</sup>) was chosen high enough to prevent the K content from masking the role of mineralogy. The N:P:K-ratio was adjusted according to Steiner (1961). The nutrient solution contained 1.83 mmol L<sup>-1</sup> Ca

$(NO_3)_2$ , 1.19 mmol L<sup>-1</sup>  $MgSO_4$ , 1.14 mmol L<sup>-1</sup> KCl, 0.52 mmol L<sup>-1</sup>  $K_2HPO_4$ , 0.44 mmol L<sup>-1</sup>  $KH_2PO_4$ , 0.20 mmol L<sup>-1</sup>  $KNO_3$ , 0.10 mmol L<sup>-1</sup>  $NH_4H_2PO_4$ ,  $4.63 \cdot 10^{-3}$  mmol L<sup>-1</sup>  $H_3BO_3$ ,  $1.64 \cdot 10^{-3}$  mmol L<sup>-1</sup>  $FeSO_4$ ,  $9.15 \cdot 10^{-4}$  mmol L<sup>-1</sup>  $MnCl_2$ ,  $8.06 \cdot 10^{-4}$  mmol L<sup>-1</sup> EDTA-Na<sub>2</sub>,  $7.65 \cdot 10^{-5}$  mmol L<sup>-1</sup>  $ZnSO_4$ ,  $5.56 \cdot 10^{-5}$  mmol L<sup>-1</sup>  $H_2MoO_4$ ,  $3.20 \cdot 10^{-5}$  mmol L<sup>-1</sup>  $CuSO_4$ . Carrier-free  $^{137}CsCl$  was added to the nutrient solution to obtain an activity concentration of about 450 kBq kg<sup>-1</sup> clay-sand mixture. The  $^{137}Cs$  spiked nutrient solution was added to the clay-sand mixture until field capacity was reached, determined by the saturated paste method (USDA, 1954). The K concentration was considered sufficiently high so that the difference in added K depending on the field capacity would be negligible. The mixture was equilibrated for three weeks prior to seeding and incubation was made at room temperature in buckets covered with a lid to prevent excessive drying, but not airtight so that conditions remained aerobic. The mixture was stirred every 2–3 days and deionized water was added to correct for weight loss.

### 2.3.2. Plant growth

Grass was sown on the  $^{137}Cs$  spiked clay-sand mixtures after separation of the pore water and one week of equilibration at field capacity (Section 2.3.3). Each mixture was divided over three pots of 1 L volume and pots were filled to obtain equal volume (D'Souza et al., 1980). Per pot, 0.65 g seeds of ryegrass (*Lolium perenne* L.) were spread on the surface and at least one centimeter from the rim so that all plant roots were evenly in contact with the mixture. The seeds were buried under 60 g of mixture. The pots were covered with a tissue to reduce drying of the top layer which was removed after the grass had germinated.

The cultivation experiment was carried out in a growing chamber with a day/night cycle of 14/10 h at 24/18 °C. The position of the pots was randomized. The pots were watered with deionized water every 2–3 days based on weight loss. The germinated grass in the Boom clay (BC) and Campine clay (CC) pots did not grow further, so watering was stopped after 18 days. Grass shoots were harvested for each of the replicate pots after 30 days. The above-ground plant material was cut off about 10 mm above surface to prevent  $^{137}Cs$  contamination from the mixture. The fresh weight of the shoots was recorded. After harvesting, the remaining grass residues were removed from the mixture. The mixture in replicate pots was put in the same bucket and air-dried.

### 2.3.3. Soil and plant analyses

Subsamples of the clay-sand mixtures were taken for measurements prior to and after plant growth. These subsamples were taken from the mixtures in buckets before plant growth and from the replicate pots combined after the pot experiment. All analyses were done in triplicate samples. The total  $^{137}Cs$  concentration in clay-sand mixture was determined on the subsamples taken from the mixtures in buckets prior to plant growth. The  $^{137}Cs$  activity was recorded with a gamma counter (1480 WIZARD 3", PerkinElmer). The pH was measured in 0.01 mol L<sup>-1</sup>  $CaCl_2$  at a S:L of 1 kg mixture to 2.5 L solution and shaken for 2 h before recording (PC 5000 L, pHenomenal®). The exchangeable K, Ca, Mg and  $^{137}Cs$  concentrations were determined by ammonium acetate ( $NH_4OAc$ ) extraction at pH 7. The mixtures were brought into contact with 1 mol L<sup>-1</sup>  $NH_4OAc$  at a S:L of 1 kg to 18 L and placed in an end-over-end shaker for 24 h. Afterwards, the supernatant was filtered at 0.45 µm. The K, Ca and Mg concentrations were measured with microwave plasma atomic emission spectroscopy (4200 MP-AES, Agilent Technologies). The  $^{137}Cs$  activity was recorded with the gamma counter. The pore water in the mixtures was separated by centrifugation at 21–23 days after spiking and incubation. The mixtures at field capacity were transferred to two-compartment cups in which the solid phase was separated by a perforated plate covered with a 2.5 µm filter (Whatman®) to collect the liquid in the lower compartment. After centrifugation, the recovered pore water was filtered at 0.45 µm and K, Ca, Mg and  $^{137}Cs$  concentrations were measured.

Pore water concentrations of K, Ca, Mg and  $^{137}Cs$  in the mixtures were measured after plant growth and air-dry storage by equilibrating the

mixture again for three weeks at field capacity and separating the pore water as described previously.

The grass shoot dry weight was recorded after drying in the oven (70 °C) for one week. The shoots were calcined (550 °C) overnight. The ash was dissolved in 2 mL of 12 mol L<sup>-1</sup> HCl, calcined again and dissolved in diluted 0.1 mol L<sup>-1</sup> HCl. The  $^{137}Cs$  concentration in solution was recorded. The K, Ca and Mg concentrations were measured after filtering the solution at 0.45 µm.

The transfer factor (TF) was calculated as the ratio of  $^{137}Cs$  concentration in the grass shoots to that in the clay-sand mixture. The concentration factor (CF), a measure of  $^{137}Cs$  plant uptake, was calculated as the ratio of  $^{137}Cs$  concentration in the grass shoots to that in the pore water.

### 2.4. Statistical analyses

The statistical analyses were performed using the JMP® Pro software (Version 16. SAS Institute Inc., Cary, NC, 1989–2022). All calculated and measured variables (except pH) were log-transformed prior to performing regression analyses. The arithmetic mean and standard deviation were calculated of the replicate samples. The TF and CF were calculated based on data of non-corresponding replicates. Therefore, standard deviations of the TF and CF were calculated based on the error of the nominator and the error of the denominator because the sampling was unpaired and no covariance was assumed. The repeatability of the data was expressed as the coefficient of variation (CV), that is the standard deviation divided by the mean. The Tukey-Kramer HSD test was performed with the significance level at 0.05 to verify the effect of clay type and dose, considered together as a treatment, on the TF replicates. Pearson correlation coefficients were calculated on the log-transformed variables (except pH) (Table A.4). Standard least squares regression and backward stepwise regression were used for two and more selected explanatory variables, respectively, to obtain relationships describing the TF.

## 3. Results and discussion

### 3.1. Selected properties of the mineral clays and deposit clays

The mineral clays and deposit clays had varying adsorption properties (Table 1). The CEC<sub>clay</sub> varied by a factor 50 and the RIP<sub>clay</sub> by a factor 22. The mineral clays had the most contrasting CEC and RIP values, while the deposit clays had values in between. All clays and deposit clays contained fractions of non-phyllosilicate minerals that were unlikely to adsorb  $^{137}Cs$ . Thus, the presence of these non-phyllosilicates diluted the weight-based RIP. Quartz, for example, is chemically inert and is negligible with respect to cation adsorption (Bellenger and Staunton, 2008). The RIP of the samples converted to RIP<sub>phyll</sub>, by dividing the value measured on the whole sample by the fraction of phyllosilicates, varied up to a factor 30 (details not shown in Table 1). This correction allowed to compare the properties of the clays with data from literature, which were usually determined on the clay fraction or pure clays.

The non-expanding phyllosilicates illite (ILL) and biotite (BIO) had a larger RIP and smaller CEC while the expanding phyllosilicates smectite (BEN) and vermiculite (VER) had a smaller RIP and larger CEC. The largest RIP value was measured for ILL, which indicated that the ILL clay had the most selective  $^{137}Cs$  adsorption sites (i.e. FES) of all the clays in this study. This was no surprise as it was known that illite strongly binds  $^{137}Cs$  (Sawhney, 1972). After correction for mineral dilution, the RIP<sub>phyll</sub> value (12,200 mmol kg<sup>-1</sup> phyllosilicates) agreed well with the RIP of pure illite (~ 10,000–16,000 mmol kg<sup>-1</sup> (de Koning, 2007; Wauters et al., 1996b)). The CEC was not markedly large compared to the other clays and the value agreed well with the CEC of illite (~ 10–40 cmol<sub>c</sub> kg<sup>-1</sup> (Grim, 1968)). The RIP of BIO was larger than previously reported (~ 1000 mmol kg<sup>-1</sup> (Eguchi et al., 2015)), and the CEC was very small compared to previously reported values (~ 35 cmol<sub>c</sub> kg<sup>-1</sup> (Fanning et al., 1989)). The BIO clay came from a rock, so it had not yet been exposed to weathering. The smallest RIP values and yet the largest CEC values were obtained for BEN and VER. The

RIP of BEN was larger than previously reported values ( $\sim 18\text{--}36 \text{ mmol kg}^{-1}$  (Ogasawara et al., 2013)), and the CEC was in the same value range ( $\sim 76 \text{ cmol}_c \text{ kg}^{-1}$  (Thiry, 1997)). The  $K_D$  of VER was previously determined in various Ca–K scenarios for purified 100–200  $\mu\text{m}$  isolated platelets ( $\sim 2500\text{--}4000 \text{ L kg}^{-1}$  for equivalent K fractions of  $<0.01\text{--}0.16$  (Thiry et al., 1996)), and the CEC was in the same range ( $\sim 144 \text{ cmol}_c \text{ kg}^{-1}$  (Thiry, 1997)). Both smectic (bentonite) and vermiculitic clays had expanded interlayers that were also accessible to monovalent as well as bivalent cations with larger hydrated radius. This interlayer surface added up to the total adsorption capacity, resulting in a large CEC compared to the other clays in this study. However, expanded clays did not bind  $^{137}\text{Cs}$  selectively to the same extent, resulting in a small RIP. We assumed that the sand used in the pot experiment was chemically inert. The sand had a CEC smaller than  $0.2 \text{ cmol}_c \text{ kg}^{-1}$  (and standard deviation  $<0.1 \text{ cmol}_c \text{ kg}^{-1}$  for  $n = 2$ ) and a RIP of  $11 \text{ mmol kg}^{-1}$  (and standard deviation  $<1 \text{ mmol kg}^{-1}$  for  $n = 3$ ). The RIP<sub>sand</sub> was a factor 35 lower than the lowest measured RIP<sub>clay</sub> (BEN). However, in a 5 % clay–sand mixture, the RIP<sub>sand</sub> could have contributed up to 35 % of the total RIP so it was defensible to include the RIP<sub>sand</sub> to determine the RIP calculated.

The RIP calculated by adding up the RIPs of the clay fraction and sand fraction (Table 1) measured before plant growth and the RIP measured on the clay–sand mixtures after plant growth agreed well ( $N = 20$ ,  $R^2 = 0.88^{***}$ , RMSE = 0.21), with a tendency of higher RIP after plant growth than before (Fig. 1). The agreement of measured and calculated RIP was not checked just before plant growth because it was assumed that mixing the clay with sand would not alter the RIP.

The agreement of the RIP measured on the separate clays and the mixtures showed that the RIP of the clays could be approximated by calculating RIP per unit of clay. However, the RIP of some clays changed during plant growth. For the BIO mixtures, the RIP measured after plant growth was about a factor 3 larger than the RIP calculated before plant growth (Fig. 1). The increase of the RIP during plant growth (e.g. BIO, ILL) was presumably due to the combination of wetting–drying cycles and plant nutrient uptake, which induced cation leaching and consequent opening of the interlayers of phyllosilicates. The interlayer opening created FES resulting in a higher RIP. Biotite has a trioctahedral structure that alters more readily than dioctahedral structures such as muscovite or illite (Bassett, 1960). For the substrates with expanding phyllosilicates (e.g. VER, BEN), the alternating factors could have led to the collapse of the interlayers, destroying FES and resulting in a smaller RIP. However, the RIP values before and after plant growth generally differed only marginally.

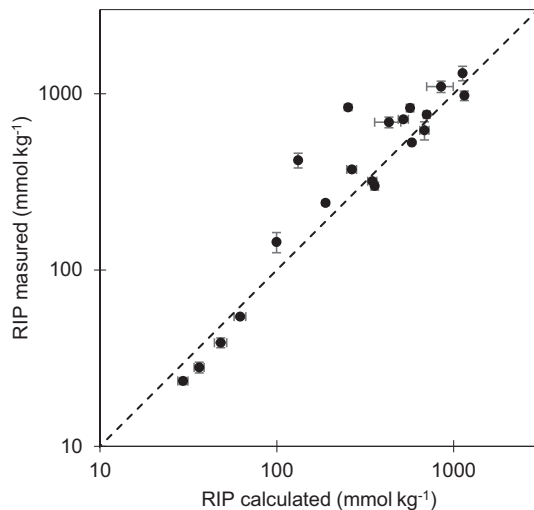


**Fig. 1.** The radio cesium interception potential (RIP) ( $\text{mmol kg}^{-1}$ ) measured on the clay–sand mixture (RIP<sub>mixture</sub>) after plant growth (y-axis) and calculated as the sum of its components RIP<sub>clay</sub> and RIP<sub>sand</sub> measured on the pure samples before mixing and plant growth (x-axis). The dashed line shows the 1:1 line. Error bars show the standard deviations ( $n = 3$ ).

### 3.2. Clay type and content controlling the $^{137}\text{Cs}$ bioavailability

The dry matter yields of grass varied within a factor 2 between the different clay–sand mixtures (Table 2), except for the BIO10 and VER10 mixtures. The Ca + Mg concentration in pore water (Table A.2) for both BIO10 and VER10 was above  $100 \text{ mmol L}^{-1}$  during plant growth, indicating that salinity affected growth. Moreover, the grass failed to grow on the BC and CC mixtures, so no data were obtained (Table 2 and Table A.3). The pH for BC and CC mixtures was below 3.5 (Table A.2), indicating that the pyrite in the mixtures oxidized during plant growth (Craen et al., 2008). Pyrite was also present in IC, but unlike on the BC and CC, the grass did grow on the IC mixtures. The carbonate minerals present in IC may have buffered the pH to above 6.5 (Table A.3).

The substrate properties influenced the  $^{137}\text{Cs}$  bioavailability. The  $^{137}\text{Cs}$  transfer factor (TF) varied widely from  $0.02 \text{ kg kg}^{-1}$  to  $2.19 \text{ kg kg}^{-1}$  (Table 2). The TF values were reproducible with limited variability among replicates ( $\text{CV} < 10\%$ , except for BIO10 (11 %) and IC20 (22 %)). The TF decreased with increasing clay content for each of the clay types (except for BIO), however the TF was not exactly halved by doubling the clay content. The K depletions in the pore water during plant growth were more pronounced at lower (5–10 wt%) than at higher (10–20 wt%) clay doses, explaining why the TF were not exactly halved by doubling the dose of clay. As expected, the RIP and exchangeable K content doubled when the clay content was doubled.

We aimed to keep the K concentration in the pore water above  $1 \text{ mmol L}^{-1}$  to minimize the effect of K on  $^{137}\text{Cs}$  bioavailability and focus on the role of the mineralogy. Unfortunately, the pore water K was below  $0.1 \text{ mmol L}^{-1}$  for some mixtures (RFC and RL, Table 2). After plant growth, the K concentration of the WC mixtures was also reduced to below  $1 \text{ mmol L}^{-1}$ . The exchangeable K content of the VER substrates was smaller than expected (Table A.2). The concentrated ammonium acetate method used to obtain the exchangeable K content may have collapsed the interlayers (de Koning and Comans, 2004) preventing the K exchange with  $\text{NH}_4^+$  cations. This is suggested by the generally larger exchangeable K contents determined using the cohext method than with the  $\text{NH}_4\text{OAc}$  method. Therefore, the exchangeable K content determined with the cohext method instead of the  $\text{NH}_4\text{OAc}$  method was used for further analyses of all substrates (Table A.2).

### 3.3. The $^{137}\text{Cs}$ bioavailability explained by pore water composition

The plant uptake of  $^{137}\text{Cs}$  from pore water, expressed by the  $^{137}\text{Cs}$  concentration factor (CF), was clearly affected by the K concentration in the pore water (Fig. 2). In a previous study on Belgian soils (Fig. 5 in Smolders et al. (1997)), the  $^{137}\text{Cs}$  concentration factor (CF) increased exponentially as the K concentration in the soil solution decreased below  $1 \text{ mmol L}^{-1}$ . The CF remained nearly the same at K concentrations above  $1 \text{ mmol L}^{-1}$  in soil solution (open symbols, Fig. 2). The CF in this experiment ranged in the same order of magnitude and was similarly related to K in solution (Fig. 2).

### 3.4. Relating $^{137}\text{Cs}$ TF to clay mineralogy and substrate properties

The factors involved in  $^{137}\text{Cs}$  transfer were statistically related to the properties of the substrate. No relation was found between the  $^{137}\text{Cs}$  TF values and the fraction of phyllosilicates ((a) in Fig. 3). However, TF was weakly and negatively related to the 2:1 type phyllosilicates (Table 3). The TF was unrelated to the 1:1 type phyllosilicates in clay–sand mixtures in which they were detected ( $N = 8$ , n.s.). The same was true for phyllosilicates of type 2:1:1 ( $N = 8$ , n.s.). The TF was weakly and negatively related to the RIP ((b) in Fig. 3 and Table 3). However, the mixtures with expanding clays BEN and VER had a distinct RIP while the TF did not differ much from the other mixtures. The relation improved if the expanding clays were omitted from the analysis ( $N = 12$ ,  $R^2 = 0.65^{**}$ ). As demonstrated before (Fig. 2), K played an important role for the fate of  $^{137}\text{Cs}$  in the soil–plant system ((c) in Fig. 3). The TF could be explained by the K concentration in pore water (Table 2) after plant growth and the

**Table 2**

Selected properties of the substrate and grass shoots *before* and *after* 30 days of plant growth. The radio cesium interception potential ( $RIP_{mixture}$ ) was measured on the clay-sand mixture after plant growth. Data are arithmetic means of replicate measurements ( $n = 3$ ) and ordered by decreasing  $^{137}\text{Cs}$  transfer factor (TF). The standard deviations of TF are given in brackets ( $n = 3$ ). The minimum, maximum and mean values are given at the bottom of the table. If no data have been obtained, “-” is noted.

Code	Mixture clay	$RIP_{mixture}$	K in pore water <i>before</i>		K in pore water <i>after</i>		Shoot		TF <sup>d</sup>	
			wt%	$\text{mmol kg}^{-1}$	$\text{mmol L}^{-1}$	$\text{mmol L}^{-1}$	Yield g	K $\text{g kg}^{-1}$		
WC	10	144	(19)	1.45	(0.02)	0.05	(<0.01)	0.72	14.3 (0.8) 2.19 <sup>a</sup> (0.04)	
WC	20	240	(8)	1.28	(0.02)	0.19	(0.01)	0.72	17.1 (1.0) 0.941 <sup>b</sup> (0.039)	
RFC	10	319	(<1)	0.12	(<0.01)	0.03	(<0.01)	0.57	11.6 (0.4) 0.641 <sup>c</sup> (0.035)	
BEN	5	23.4	(1.1)	5.02	(0.06)	2.15	(0.04)	0.85	21.3 (0.7) 0.625 <sup>e</sup> (0.038)	
BEN	10	38.7	(2.4)	6.99	(0.13)	5.22	(0.11)	0.72	30.7 (0.6) 0.371 <sup>d</sup> (0.020)	
RL	10	299	(15)	0.08	(<0.01)	0.04	(<0.01)	0.57	8.7 (0.7) 0.369 <sup>d</sup> (0.032)	
BIO	10	837	(33)	16.09	(0.59)	13.05	(0.74)	0.36	31.2 (2.2) 0.351 <sup>d</sup> (0.038)	
VER	5	28.0	(2.0)	1.44	(0.06)	1.23	(0.03)	0.60	25.5 (2.0) 0.333 <sup>d,e</sup> (0.014)	
BIO	5	420	(40)	9.47	(0.18)	3.64	(0.04)	0.70	24.8 (2.3) 0.294 <sup>d,e</sup> (0.029)	
RFC	20	620	(73)	0.07	(<0.01)	0.03	(<0.01)	0.76	13.7 (0.6) 0.268 <sup>e</sup> (0.007)	
VER	10	54.4	(1.2)	3.65	(0.09)	2.26	(0.04)	0.34	30.1 (2.1) 0.183 <sup>f</sup> (0.013)	
RL	20	761	(14)	0.06	(<0.01)	0.04	(0.01)	0.65	11.8 (0.9) 0.168 <sup>f</sup> (0.010)	
ILL	5	689	(48)	6.58	(0.11)	2.94	(0.02)	0.74	25.6 (1.4) 0.0524 <sup>g</sup> (0.0015)	
ILL	10	1100	(80)	9.14	(0.12)	5.68	(0.10)	0.71	26.4 (1.0) 0.0435 <sup>g</sup> (0.0025)	
IC	10	528	(12)	6.11	(0.17)	4.28	(0.10)	0.72	19.4 (2.1) 0.0324 <sup>h</sup> (0.0034)	
IC	20	975	(61)	6.58	(0.12)	5.42	(0.31)	0.86	20.2 (3.0) 0.0151 <sup>i</sup> (0.0034)	
BC	10	830	(41)	5.90	(0.17)	-	-	-	-	
BC	20	1310	(120)	6.24	(0.15)	-	-	-	-	
CC	10	372	(13)	0.67	(0.06)	-	-	-	-	
CC	20	715	(17)	0.28	(0.02)	-	-	-	-	
min		23.4		0.06		0.03		0.34	8.7 0.0151	
max		1310		16.09		13.05		0.86	31.2 2.19	
median		474		4.34		2.20		0.72	20.8 0.313	

<sup>d</sup> Italicized superscript letter refers to Tukey-Kramer HSD connecting letters of log TF that are no different at  $p < 0.05$ .

$RIP_{mixture}$  ((d) in Fig. 3). The RIP to pore water K ratio is the  $^{137}\text{Cs}$   $K_D$  based on a simplified formula (Wauters et al., 1996c) assuming that the concentrations of  $\text{NH}_4$  and Na in pore water are low enough to be neglected.

The effect of the K concentration in the pore water on the fate of  $^{137}\text{Cs}$  can be observed graphically as a shift of the TF value to a higher level when the K concentration in the pore water is below a certain threshold level for mixtures with similar RIP-K ratios ((d) Fig. 3). The field capacity is not a significant estimator for the TF value, which proves that the effect of variable doses of K dependent on the field capacity was negligible.

The  $^{137}\text{Cs}$  TF could be predicted based on the mechanisms of K competition and the  $^{137}\text{Cs}$  selective adsorption. The TF could be predicted in a multiple linear regression with the  $RIP_{mixture}$  and the K concentration in the pore water (Table 3), which logically followed from the important

roles of sorption and ion competition effects as showed in the analysis of soil solution based TF prediction (Figs. 2 and 3d). The TF prediction improved if instead of the pore water K, the exchangeable K content was considered (Table 3), which reflected the K buffering capacity.

The RIP is a soil property that is not reflected in general purpose soil maps while the mineralogy may be inferred from soil classification. Hence, the mineralogy was put forward as an estimator for FES and K buffering capacity with a view to upgrade soil maps with FES and K buffering capacity derived from available soil information for each mapping unit. Logically, the  $^{137}\text{Cs}$  selective adsorption could not be described by the total phyllosilicate content and the TF was not significantly affected by total clay content (Fig. 3a). The 2:1 phyllosilicate content correlated negatively to the TF, but the correlation was poor (Table 3). More detailed information of the 2:1 clay types (Table A.1) better explained the TF and the best model was reached with  $R^2 = 0.74$  when four different clay mineral fractions were used (Table 3). In that best model, the parameter values for each of the three different 2:1 clay fractions (log transformed) were similar and not different from 1, so there was a proportional decrease in TF when these fractions increased. Most strikingly, there was a statistically positive effect of 1:1 clays, indicating that these clay fractions enhanced  $^{137}\text{Cs}$  bioavailability which was against expectation as these clays, devoid of FES, were expected to have no effect on the TF.

The regression models based on the exchangeable K content or 2:1 phyllosilicates derived here (Table 3) were compared to existing TF prediction models for soil. A TF model for grass created for mineral soils (Absalom et al., 1999) had contact time (58 days with  $^{137}\text{Cs}$ ), exchangeable K content and total phyllosilicate content as predictor variables. The total phyllosilicate content, which is the sum of the 1:1, 2:1, and 2:1:1 clays, was chosen instead of clay content because of the presence of non-phyllosilicates discussed earlier (Section 3.1). That TF model performed barely better ( $R^2 = 0.59^{***}$ , RMSE = 0.38, details not shown) compared to the exchangeable K content regression model (Table 3). When instead of the total phyllosilicate level in the existing model, the 2:1 phyllosilicate content was considered, the model performance did not improve ( $R^2 = 0.57^{***}$ , RMSE = 0.39). The other model adjusted for organic soils (Absalom et al., 2001) performed worse and largely underestimated  $^{137}\text{Cs}$  transfer, presumably because it was calibrated on soils with a higher

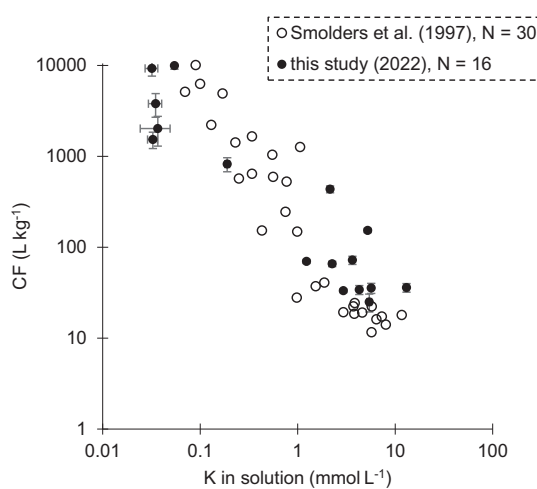


**Fig. 2.** Graph showing how the K concentration in solution affected the  $^{137}\text{Cs}$  plant uptake. The plant shoot to soil solution  $^{137}\text{Cs}$  concentration ratio, that is the concentration factor ( $\text{CF}, \text{L kg}^{-1}$ ), increased when the K concentration in solution ( $\text{mmol L}^{-1}$ ) for pore water conditions after plant growth decreased below 1  $\text{mmol L}^{-1}$ . Error bars show the standard deviations ( $n = 3$ ).

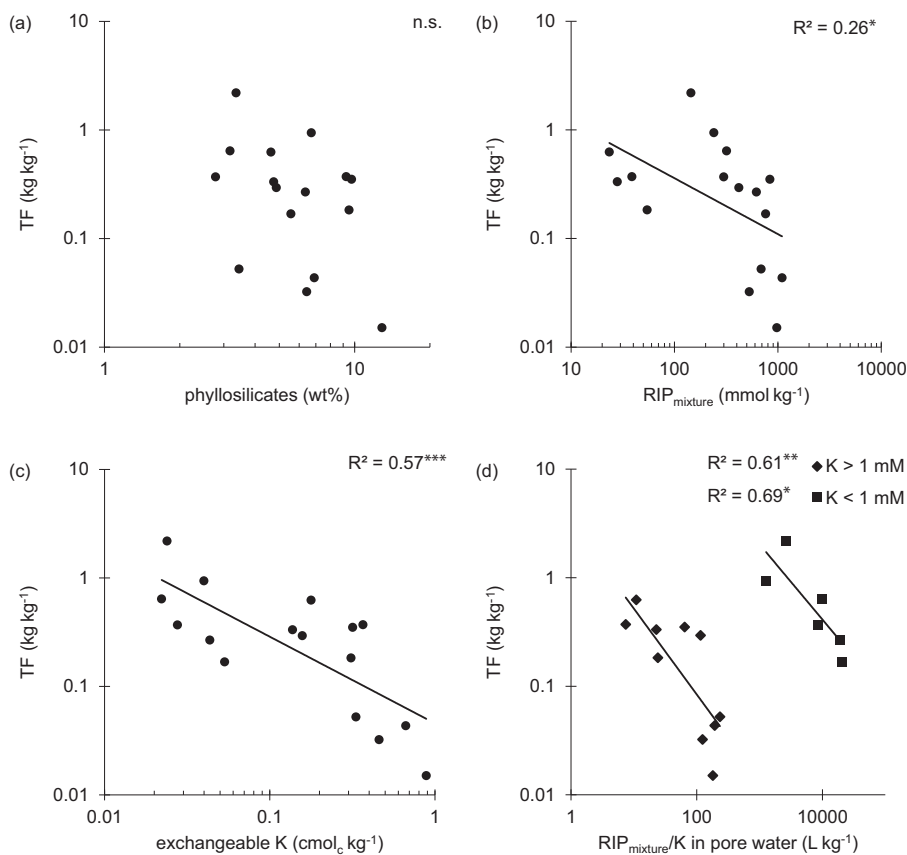


**Fig. 3.** The  $^{137}\text{Cs}$  transfer factor (TF) ( $N = 16$ ) predicted by (a) the fraction of phyllosilicates in the clay-sand mixtures (b) the RIP of the clay-sand mixtures measured after plant growth (c) the cohex exchangeable K content (d) the ratio of the RIP of the clay-sand mixtures to the K concentration in pore water after plant growth. The points on the graph are mean TF values ( $n = 3$ ).

content of organic matter. The updated model predictions of  $^{137}\text{Cs}$  transfer (Tarsitano et al., 2011) had a smaller error compared to the older model versions ( $R^2 = 0.53^{**}$ , RMSE = 0.41). Our finding is that the inclusion of XRD-based information could improve the model if the structure of the model is changed and recalibrated.

**Table 3**

Statistical models relating the transfer factors (TF in  $\text{kg kg}^{-1}$ ) to the clay mineralogy and substrate properties ( $N = 16$ ). Models are sorted by increasing  $R^2$  and decreasing Root Mean Square Error. Parameter uncertainties are standard error in brackets.  $\text{RIP}_{\text{mixture}}$  is expressed in  $\text{mmol kg}^{-1}$ , %2:1 is the total 2:1 phyllosilicate content in wt%, %di2:1 is the dioctahedral 2:1 phyllosilicate content of illite or smectite (subscript) in wt%, %tri2:1 is the trioctahedral 2:1 phyllosilicate content in wt%, %1:1 is the total 1:1 phyllosilicate content in wt%, K is the K concentration in pore water after growth in  $\text{mmol L}^{-1}$  and ex K is the cohex exchangeable K content in  $\text{cmolc kg}^{-1}$ .

Model equation	$R^2$	RMSE
$\log(\text{TF}) = 0.58(0.57) - 0.51(0.23)\log(\text{RIP}_{\text{mixture}})$	0.26*	0.51
$\log(\text{TF}) = 0.26(0.38) - 1.35(0.52)\log(\%2:1)$	0.32*	0.49
$\log(\text{TF}) = -2.69(0.60) - 0.51(0.17)\log(\%\text{di2:1}_{\text{ill}}) - 1.02(0.31)\log(\%\text{di2:1}_{\text{sme}}) - 1.14(0.34)\log(\%\text{tri2:1})$	0.53*	0.44
$\log(\text{TF}) = 0.61(0.46) - 0.54(0.19)\log(\text{RIP}_{\text{mixture}}) - 0.31(0.11)\log(\text{K})$	0.54**	0.42
$\log(\text{TF}) = -1.34(0.19) - 0.80(0.19)\log(\text{ex K})$	0.58***	0.39
$\log(\text{TF}) = -2.42(0.48) - 0.87(0.18)\log(\%\text{di2:1}_{\text{ill}}) - 1.06(0.25)\log(\%\text{di2:1}_{\text{sme}}) - 1.14(0.27)\log(\%\text{tri2:1}) + 0.53(0.18)\log(\%\text{1:1})$	0.74***	0.35
$\log(\text{TF}) = -0.22(0.37) - 0.45(0.14)\log(\text{RIP}_{\text{mixture}}) - 0.76(0.14)\log(\text{ex K})$	0.76***	0.30

\*  $p < 0.05$ .

\*\*  $p < 0.01$ .

\*\*\*  $p < 0.001$ .

#### 4. Conclusion

Our pot cultivation experiment showed that both the amount and type of phyllosilicates in a substrate have an important role on the  $^{137}\text{Cs}$  bioavailability, with a logical effect of the type of mineral clays (illite, biotite, smectite or vermiculite) that affect the bioavailability. The TF cannot be predicted with a regression model based on the exchangeable K level and 2:1 type phyllosilicates. However, differentiating the 2:1 type clays explained the TF in statistical terms but it is likely that this advanced XRD is unfeasible for routine analysis of soils, let be that it can be combined with existing soil map information for geospatial assessments. The existing models predicted the TF little or no better than a simple regression model of only the exchangeable K content. Further research on natural soils across different parent rocks and weathering stages is required to reveal to what extent XRD based soil mineralogy can predict  $^{137}\text{Cs}$  bioavailability.

#### CRediT authorship contribution statement

**Margot Vanheukelom:** Conceptualization, Formal analysis, Investigation, Methodology, Validation, Visualization, Writing – original draft, Writing – review & editing. **Lieve Sweeck:** Conceptualization, Funding acquisition, Investigation, Methodology, Project administration, Resources, Supervision, Validation, Writing – review & editing. **May Van Hees:** Data curation, Formal analysis, Methodology. **Nancy Weyns:** Data curation, Formal analysis, Methodology. **Jos Van Orshoven:** Conceptualization, Funding acquisition, Project administration, Resources, Supervision, Writing – original draft, Writing – review & editing. **Erik Smolders:** Conceptualization, Supervision, Visualization, Writing – original draft, Writing – review & editing.

## Data availability

I have shared the link to my data/code at the Attach File step  
[Vanheukelom2022\\_XRD-pattern \(Original data\)](#) (Mendeley Data)

## Declaration of competing interest

The authors declare that they have no known competing financial interests or personal relationships that could have appeared to influence the work reported in this paper.

## Appendix A

The RIP of reference illite du Puy is 4397 mmol kg<sup>-1</sup> (and standard deviation 88 mmol kg<sup>-1</sup>) and the CEC is 18.0 cmol<sub>c</sub> kg<sup>-1</sup> (and standard deviation 0.5 cmol<sub>c</sub> kg<sup>-1</sup>).

The group of 2:1 structure phyllosilicates consists both of the very selective, non-expanding and less selective, expanding minerals. As suggested by Zeelmaekers (2011), we quantify the 2:1 phyllosilicates and group them together, however XRD cannot detect FES and hence, 2:1 phyllosilicates refer to high and low RIP clays. This is because it is challenging to distinguish the 2:1 phyllosilicates with XRD. The XRD technique relies on the identification of the mineral interlayer spaces, which in case of the phyllosilicates have a closely matching distance so that characteristic peaks often overlap. By isolating the phyllosilicates, the type 2:1 phyllosilicates can be distinguished. However, this additional information is often too laborious to obtain in a routine manner. The isolation of the phyllosilicates prior to the XRD analysis was done following the standardized procedure suggested by Zeelmaekers (2011) as given below.

The fraction smaller than 2 µm was isolated after chemical removal of aggregate forming particles and centrifugation (modified after Jackson, 1975; Zeelmaekers, 2011). The clays were chemically treated to remove cements that hold clay particles in a matrix. Carbonates were removed by a pH 5 buffer solution of Na-acetate and acetic acid. The organic matter was oxidized by a 7 % H<sub>2</sub>O<sub>2</sub> solution. Free iron (hydr)oxides were removed by a citrate-bicarbonate-dithionite solution. The clays were ultrasonically treated to loosen the aggregates between each treatment. The 2 µm fraction was separated by centrifuging the clays at 305 g for 2 min. The interlayers were saturated by calcium ions by dissolving the clays in a 1 mol L<sup>-1</sup> CaCl<sub>2</sub> solution to ensure interlayer conditions were similar. Excess chloride ions were removed by placing the clays in a dialysis membrane (VISKING®, MWCO 12 kDa to 14 kDa) in deionized water which was refreshed twice a day for 5 days. Afterwards the clays were dried in the oven (60 °C) overnight.

The 00̄l reflections of the phyllosilicate minerals were enhanced by depositing the isolated phyllosilicates on a glass slide prior to XRD measurements. The oven-dry clays were dispersed in deionized water after ultrasonic treatment. About 10 mg of clay per cm<sup>2</sup> was deposited on the glass slide (Moore and Reynolds, 1997). The slides were recorded with XRD in two states: air-dry and solvated in ethylene glycol. After the air-dried slide was measured, the slide was inserted in a desiccator with ethylene glycol bath in an oven (60 °C) overnight. The slides in two states were measured with the same diffractometer as described above, but with a scanning range from 2°20 to 47°20.

The minerals in the isolated 2 µm fraction were identified and quantified using SYBILLA (© Chevron ETC). The SYBILLA software, based on the multispecimen method, fits the model on the XRD record in two states (Zeelmaekers, 2011). The quantified phase results were accepted if the model fit in the ethylene glycol state agreed with the model in the air-dry state.

The VER pattern of the isolated clay fraction was impossible to quantify with the SYBILLA software. It is known that vermiculite and vermiculite-chlorite mixed minerals are present in VER (Thiry, 1997). However, the vermiculite and chlorite minerals were quantified in the bulk sample, so it did not affect the final conclusion based on 2:1 and 2:1:1 groups of summed mineral phases.

The results from both bulk rock analysis and the isolated clay fraction were combined as explained by Zeelmaekers (2011). The isolated clay results were integrated by splitting the bulk-rock quantity for the 2:1 type group into proportions of illite, smectite and interstratified illite-smectite according to their relative proportions in the isolated 2 µm fraction. After the identified mineral phases were quantified, the results were normalized.

**Table A.1**

The mineral content (wt%) of the quantified mineral phases after XRD analysis. The group of Al-rich dioctahedral 2:1 phyllosilicates is split up in illite, illite-smectite mixed layered and smectite mineral contents. The data are arithmetic means if replicates in the bulk powder method were measured (*n* = 1, 3 or 4, see below).

Minerals	BEN <sup>e</sup>	BIO <sup>e</sup>	ILL <sup>e</sup>	VER <sup>e</sup>	BC <sup>f</sup>	CC <sup>g</sup>	IC <sup>g</sup>	RFC <sup>f</sup>	RL <sup>f</sup>	WC <sup>f</sup>
Illite	<0.1	<0.1	42.5	<0.1	4.0	5.1	5.7	6.9	2.4	9.3
Illite-smectite	<0.1	<0.1	24.5 <sup>h</sup>	<0.1	14.1 <sup>h</sup>	14.0 <sup>h</sup>	8.8 <sup>h</sup>	7.6 <sup>h</sup>	9.1 <sup>h</sup>	6.4 <sup>i</sup>
Smectite	92.6	<0.1	<0.1	<0.1	27.2	9.3	40.6	11.0	11.3	<0.1
Fe-rich dioctahedral 2:1 phyllosilicates	<0.1	<0.1	<0.1	<0.1	<0.1	<0.1	<0.1	<0.1	<0.1	<0.1
Fe-rich trioctahedral 2:1 phyllosilicates	<0.1	97.3	<0.1	86.0	<0.1	<0.1	<0.1	<0.1	<0.1	<0.1
Kaolinite	<0.1	<0.1	1.0	<0.1	6.2	3.4	4.4	1.3	1.1	18.0
Kaolinite-smectite	<0.1	<0.1	<0.1	<0.1	4.2	3.5	2.0	2.4	1.9	<0.1
Chloritic minerals	<0.1	<0.1	1.0	9.0	2.0	3.3	2.9	2.7	2.0	<0.1
Quartz	3.0	<0.1	21.0	<0.1	28.8	52.1	22.5	58.5	53.0	64.2
K-feldspar	3.0	<0.1	8.0	<0.1	7.7	5.0	6.6	4.7	8.3	1.5
Plagioclase	1.0	<0.1	<0.1	<0.1	2.7	2.8	3.5	5.0	9.3	<0.1
Augite	<0.1	<0.1	<0.1	4.0	<0.1	<0.1	<0.1	<0.1	<0.1	<0.1

**Table A.1** (continued)

Minerals	BEN <sup>e</sup>	BIO <sup>e</sup>	ILL <sup>e</sup>	VER <sup>e</sup>	BC <sup>f</sup>	CC <sup>g</sup>	IC <sup>g</sup>	RFC <sup>f</sup>	RL <sup>f</sup>	WC <sup>f</sup>
Carbonate minerals	0.4	<0.1	2.0	1.0	<0.1	<0.1	0.8	<0.1	1.7	<0.1
Gypsum	<0.1	<0.1	<0.1	<0.1	0.8	0.9	0.6	<0.1	<0.1	<0.1
Apatite	<0.1	2.7	<0.1	<0.1	<0.1	<0.1	<0.1	<0.1	<0.1	<0.1
Pyrite	<0.1	<0.1	<0.1	<0.1	1.7	0.3	1.0	<0.1	<0.1	<0.1
Anatase	<0.1	<0.1	<0.1	<0.1	0.6	0.3	0.7	<0.1	<0.1	<0.1
Rutile	<0.1	<0.1	<0.1	<0.1	<0.1	<0.1	<0.1	<0.1	<0.1	0.7

<sup>e</sup> n = 1.<sup>f</sup> n = 3.<sup>g</sup> n = 4.<sup>h</sup> Randomly interstratified.<sup>i</sup> Regularly interstratified.

The 'CEC calculated' of the sand-clay mixtures was calculated as for the RIP calculated (Section 2.2.2). The agreement of the CEC measured on the clays and the mixtures shows the CEC additivity ( $N = 20$ ,  $R^2 = 0.92^{***}$ , RMSE = 0.13) (Fig. A.1). In mineral substrates, residual CEC is negligible. However, in soils where there is organic matter, this can be a large part of the non-selective adsorption.

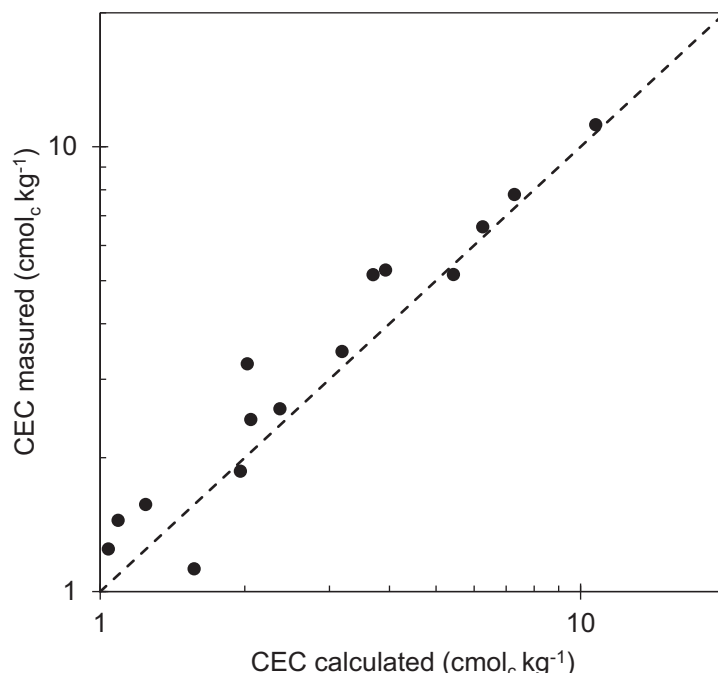


**Fig. A.1.** The cation exchange capacity (CEC) (cmolc kg<sup>-1</sup>) measured on the clay-sand mixture before plant growth (x-axis) and calculated as the sum of the CEC of its component clay and sand (y-axis). The dashed line shows the 1:1 line.

Data is given of the measured variables prior (Table A.2) and after (Table A.3) plant growth.

**Table A.2**  
Properties of the substrate and grass shoots before plant growth. Data are arithmetic means and standard deviations (in parentheses) of triplicates, unless stated otherwise. The standard deviation of RIP calculated is calculated based on the error of the RIP<sub>day</sub> and RIP<sub>sand</sub> and no covariance is assumed. The minimum, maximum and mean values are given at the bottom of the table.

Code	Substrate	Exchangeable cations			Pore water			RIP <sub>calculated</sub>						
		CEC <sup>j</sup> cmol <sub>c</sub> kg <sup>-1</sup>	Moisture content g H <sub>2</sub> O 100 g <sup>-1</sup>	pH (0.01 M CaCl <sub>2</sub> )	Total <sup>137</sup> Cs kBq kg <sup>-1</sup>	<sup>137</sup> Cs kBq kg <sup>-1</sup>	K <sup>i</sup> (cohex) cmol <sub>c</sub> kg <sup>-1</sup>	Ca (NH <sub>4</sub> OAc) cmol <sub>c</sub> kg <sup>-1</sup>	Mg (NH <sub>4</sub> OAc) cmol <sub>c</sub> kg <sup>-1</sup>	Ca mmol L <sup>-1</sup>	Mg mmol L <sup>-1</sup>			
BENS	5.2	21.3	7.7 (0.1)	396.4 (5.9)	231 (7.0)	0.18	0.22 (<0.01)	6.0 (0.2)	2.0 (<0.1)	18.3 (0.18)	5.02 (0.06)	44.32 (0.58)	13.1 (0.20)	29.5 (2.0)
BEN10	7.8	27.2	7.6 (<0.1)	405.6 (5.9)	207 (1.8)	0.37	0.40 (0.02)	11.5 (0.8)	3.0 (0.1)	12.0 (0.53)	6.99 (0.13)	76.81 (1.20)	22.7 (0.40)	48.2 (3.9)
BIO5	0.6	13.3	8.5 (<0.1)	413.0 (1.6)	90.9 (2.8)	0.16	0.21 (<0.01)	3.8 (0.1)	0.6 (<0.1)	11.1 (0.68)	9.47 (0.18)	41.62 (0.36)	14.5 (0.33)	13.2 (2)
BIO10	0.2	13.6	8.3 (0.1)	405.8 (5.0)	77.2 (0.2)	0.32	0.40 (<0.01)	8.6 (<0.1)	1.1 (<0.1)	9.6 (0.27)	16.09 (0.59)	80.95 (2.16)	26.5 (0.66)	25.3 (4)
ILL5	1.6	12.8	8.0 (<0.1)	385.2 (0.4)	115 (2.0)	0.33	0.36 (<0.01)	4.9 (0.1)	3.0 (0.1)	1.69 (0.08)	6.58 (0.11)	32.78 (0.51)	9.69 (0.18)	43.0 (73)
ILL10	2.6	16.0	7.9 (<0.1)	378.9 (10.0)	110 (1.1)	0.67	0.74 (<0.01)	9.8 (0.1)	5.8 (<0.1)	1.34 (0.03)	9.14 (0.12)	51.53 (0.59)	17.6 (0.58)	85.0 (145)
VER5	5.2	13.4	8.0 (<0.1)	402.1 (5.9)	17.3 (0.9)	0.14	0.06 (<0.01)	4.9 (0.2)	4.1 (0.1)	2.34 (0.45)	1.44 (0.06)	21.39 (1.09)	11.1 (0.45)	36.4 (2.4)
VER10	11.2	13.2	7.8 (0.1)	392.1 (10.5)	11.0 (0.6)	0.31	0.10 (<0.01)	9.4 (0.5)	7.7 (0.3)	1.24 (0.29)	3.65 (0.09)	72.76 (1.13)	44.2 (0.23)	62.0 (4.7)
BC10	3.2	13.5	3.2 (<0.1)	388.3 (12.1)	176 (17.0)	0.32	0.14 (<0.01)	3.4 (0.3)	1.2 (0.1)	1.45 (0.13)	13.56 (0.17)	13.56 (0.13)	21.4 (0.83)	56.7 (10)
BC20	5.3	16.2	2.9 (0.1)	402.8 (7.5)	143 (7.8)	0.61	0.39 (0.02)	6.6 (0.4)	2.4 (0.2)	0.75 (0.04)	6.24 (0.15)	13.23 (0.06)	26.9 (0.74)	112.0 (20)
CC10	1.4	13.3	3.0 (0.1)	394.1 (8.7)	236 (19.0)	0.05	0.04 (<0.01)	1.9 (0.2)	0.3 (<0.1)	1.19 (0.01)	0.67 (0.06)	13.97 (0.19)	6.75 (0.19)	26.6 (17)
CC20	1.1	13.5	2.9 (0.1)	391.2 (3.0)	202 (9.7)	0.09	0.06 (<0.01)	2.8 (0.1)	0.6 (<0.1)	0.55 (0.01)	0.28 (0.02)	12.50 (0.04)	12.2 (0.34)	52.0 (34)
IC10	3.5	13.1	6.8 (0.2)	370.9 (17.3)	128 (7.4)	0.46	0.51 (0.01)	4.0 (<0.1)	2.4 (<0.1)	0.95 (0.11)	6.11 (0.17)	15.42 (0.30)	13.3 (0.80)	58.1 (17)
IC20	6.6	18.9	6.8 (0.2)	410.5 (16.2)	118 (5.2)	0.89	0.98 (0.04)	7.2 (0.4)	4.3 (0.2)	0.55 (0.04)	6.58 (0.12)	15.63 (0.25)	13.7 (1.16)	115.0 (30)
RFC10	1.2	11.0	7.1 (0.1)	378.8 (6.6)	85.9 (10.5)	0.02	0.03 (<0.01)	1.5 (0.2)	0.1 (<0.1)	0.10 (0.01)	0.12 (<0.01)	4.42 (0.08)	0.66 (0.01)	34.7 (20)
RFC20	1.9	13.2	6.6 (0.2)	391.6 (9.2)	73.1 (5.6)	0.04	0.05 (<0.01)	2.3 (0.1)	0.2 (<0.1)	0.05 (0.02)	0.07 (<0.01)	4.45 (0.07)	0.59 (<0.01)	68.4 (41)
RL10	1.4	10.7	7.6 (<0.1)	399.3 (7.1)	102 (3.0)	0.03	0.05 (<0.01)	9.3 (0.3)	0.4 (<0.1)	0.06 (0.01)	0.08 (<0.01)	4.31 (0.16)	0.35 (0.01)	35.7 (15)
RL20	2.4	10.8	7.4 (0.1)	403.9 (8.2)	98.4 (3.8)	0.05	0.09 (0.01)	16.7 (0.6)	0.4 (<0.1)	0.05 (0.01)	0.06 (<0.01)	4.75 (0.05)	0.32 (0.01)	70.4 (29)
WC10	0.5	12.0	6.6 (<0.1)	406.8 (7.2)	189 (0.8)	0.02	0.03 (<0.01)	0.7 (<0.1)	0.2 (<0.1)	0.21 (0.11)	1.45 (0.02)	8.09 (0.23)	2.44 (0.05)	100 (2)
WC20	0.6	13.1	6.5 (0.1)	404.1 (4.6)	191 (2.1)	0.04	0.04 (<0.01)	1.0 (0.1)	0.3 (<0.1)	0.78 (0.05)	1.28 (0.02)	11.40 (0.44)	3.76 (0.07)	189 (3)
min	0.2	10.7	2.9	370.9	11.0	0.02	0.03	0.7	0.1	0.05	0.06	4.31	0.32	29.5
max	11.2	27.2	8.5	413.0	236	0.90	0.98	16.7	7.7	18.33	16.09	80.95	44.2	115.0
median	2.2	13.3	7.2	397.9	116	0.17	0.11	4.9	1.2	4.34	14.70	352	12.7	

j n = 1.

**Table A.3**

Properties of the substrate and grass shoots after 30 days of plant growth. Data are arithmetic means and standard deviations (in parentheses) of triplicates. The CF is calculated based on data of non-corresponding replicates. Therefore, standard deviations of the CF is calculated based on the error of the nominator and the error of the denominator because the sampling is unpaired and no covariance is assumed. The minimum, maximum and mean values are given at the bottom of the table. If no data have been obtained, a “-” is noted.

Code	Pore water				Grass shoot								RIP <sub>mixture</sub> mmol kg <sup>-1</sup>	CF L kg <sup>-1</sup>
	<sup>137</sup> Cs kBq L <sup>-1</sup>	K mmol L <sup>-1</sup>	Ca mmol L <sup>-1</sup>	Mg mmol L <sup>-1</sup>	yield g	<sup>137</sup> Cs kBq kg <sup>-1</sup>	K g kg <sup>-1</sup>	Ca g kg <sup>-1</sup>	Mg g kg <sup>-1</sup>					
BEN5	0.57 (0.04)	2.15 (0.04)	39.26 (0.51)	10.67 (0.20)	0.85 (0.07)	247.9 (14.5)	21.3 (0.7)	15.1 (1.2)	2.2 (0.1)	23 (1)	435 (38)			
BEN10	0.98 (0.01)	5.22 (0.11)	70.68 (2.45)	20.35 (0.46)	0.72 (0.08)	150.5 (8.0)	30.7 (0.6)	19.9 (4.8)	2.8 (0.6)	39 (2)	153 (8)			
BIO5	1.68 (0.05)	3.64 (0.04)	30.14 (0.11)	9.85 (0.12)	0.70 (0.09)	121.4 (12.0)	24.8 (2.3)	16.9 (0.6)	2.7 (0.1)	420 (40)	72.1 (7.4)			
BIO10	3.96 (0.08)	13.05 (0.74)	82.49 (3.28)	28.93 (1.79)	0.36 (0.01)	142.4 (15.1)	31.2 (2.2)	22.2 (4.3)	3.3 (0.3)	837 (33)	35.9 (3.9)			
ILL5	0.61 (0.02)	2.94 (0.02)	24.62 (0.02)	7.64 (0.05)	0.74 (0.03)	20.2 (0.6)	25.6 (1.4)	14.8 (1.5)	2.5 (0.1)	689 (48)	33.2 (1.4)			
ILL10	0.46 (0.05)	5.68 (0.10)	42.06 (0.67)	13.43 (0.08)	0.71 (0.02)	16.5 (0.8)	26.4 (1.0)	17.2 (1.2)	2.5 (0.1)	1097 (82)	35.6 (4.5)			
VER5	1.92 (0.05)	1.23 (0.03)	25.72 (0.18)	16.03 (0.10)	0.60 (0.03)	133.9 (5.4)	25.5 (2.0)	19.1 (1.0)	4.1 (0.2)	28 (2)	69.8 (3.4)			
VER10	1.09 (0.03)	2.26 (0.04)	62.01 (0.62)	39.33 (0.60)	0.34 (0.06)	71.8 (4.6)	30.1 (2.1)	28.0 (1.4)	6.1 (0.3)	54 (1)	65.7 (4.5)			
BC10	-	-	-	-	-	-	-	-	-	830 (41)	-	-	-	
BC20	-	-	-	-	-	-	-	-	-	1307 (123)	-	-	-	
CC10	-	-	-	-	-	-	-	-	-	372 (13)	-	-	-	
CC20	-	-	-	-	-	-	-	-	-	715 (17)	-	-	-	
IC10	0.35 (0.02)	4.28 (0.10)	15.05 (0.47)	11.58 (0.27)	0.72 (0.02)	12.0 (1.1)	19.4 (2.1)	5.7 (0.4)	2.8 (0.2)	528 (12)	34.0 (3.9)			
IC20	0.25 (0.01)	5.42 (0.31)	15.30 (0.25)	13.98 (0.67)	0.86 (0.04)	6.2 (1.4)	20.2 (3.0)	5.0 (0.6)	2.8 (0.2)	975 (61)	25.0 (5.6)			
RFC10	0.03 (<0.01)	0.03 (<0.01)	2.02 (0.03)	0.20 (0.01)	0.57 (0.04)	242.7 (12.4)	11.6 (0.4)	14.5 (0.2)	2.8 (0.2)	318.9 (<1)	9250 (1630)			
RFC20	0.07 (0.01)	0.03 (<0.01)	2.15 (0.05)	0.20 (0.01)	0.76 (0.04)	104.9 (1.5)	13.7 (0.6)	12.7 (0.3)	2.4 (0.1)	620 (73)	1530 (310)			
RL10	0.04 (0.01)	0.04 (<0.01)	2.27 (0.06)	0.12 (0.01)	0.57 (0.05)	147.4 (12.6)	8.7 (0.7)	8.9 (0.3)	1.5 (0.1)	299 (15)	3790 (1100)			
RL20	0.03 (0.01)	0.04 (0.01)	2.24 (0.02)	0.11 (0.02)	0.65 (0.01)	68.1 (3.9)	11.8 (0.9)	9.5 (0.5)	1.7 (0.2)	761 (14)	2020 (730)			
WC10	0.09 (0.01)	0.05 (<0.01)	5.78 (0.19)	1.64 (0.08)	0.72 (0.03)	891.7 (8.8)	14.3 (0.8)	10.2 (0.2)	2.5 (<0.1)	144 (19)	9940 (860)			
WC20	0.46 (0.08)	0.19 (0.01)	9.34 (0.40)	3.10 (0.08)	0.72 (0.04)	380.1 (15.3)	17.1 (1.0)	9.4 (0.3)	2.3 (0.2)	240 (8)	821 (145)			
min	0.03	0.03	2.02	0.11	0.34	6.2	8.7	5.0	1.5	23	25.0			
max	3.96	13.05	82.49	39.33	0.86	891.7	31.2	28.0	6.1	1307	9940			
median	0.46	2.20	19.96	10.26	0.72	127.7	20.8	14.7	2.6	474	112			

The K concentrations in pore water were similar before and after plant growth (Fig. A.2). The concentrations of <sup>137</sup>Cs were reduced during the pot experiment. The large <sup>137</sup>Cs concentration changes in the pore water of BEN and BIO substrates cannot be ascribed to a depletion in K ions competing for <sup>137</sup>Cs adsorption on the solid phase which can be shown by mass balance calculations. Plant uptake also cannot explain the largest concentration changes because the total estimated plant accumulation of <sup>137</sup>Cs was <10 % of the quantify initially present in pore water if the above ground part is assumed 2/3 of the total biomass. This agrees with what was found earlier (Smolders et al., 1997) after which it was concluded that both pore water cation concentrations before or after plant growth could be used to demonstrate relationships such as the influence of pore water composition on <sup>137</sup>Cs availability.

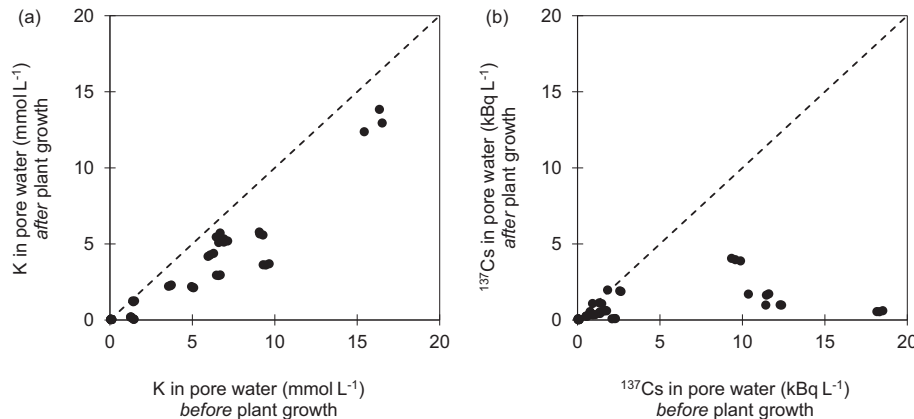


**Fig. A.2.** The change in pore water concentrations before (x-axis) and after (y-axis) plant growth for (a) K and (b) <sup>137</sup>Cs. Replicate values are shown. The dashed line shows the 1:1 line.

It is expected that the large <sup>137</sup>Cs concentration changes in pore water is due to a low capacity to selectively bind <sup>137</sup>Cs. However, although BEN with the lowest RIP of all substrates explains the <sup>137</sup>Cs depletion in the pore water, this is not the case for the BIO substrate which has a larger RIP that increases during the pot experiment. The change in both the available <sup>137</sup>Cs in the pore water and the selective adsorption of <sup>137</sup>Cs onto the solid phase has implications on the assumption that the <sup>137</sup>Cs soil-pore water ratio, that is the solid-liquid distribution coefficient  $K_D$ , may be considered constant during the course of the experiment, although this is only for two exceptional cases BEN and BIO substrates.

The behavior of Cs in the soil-plant system is described by a sorption-desorption process between soil and solution, quantified by  $K_D$ , and an ion uptake process from solution to plant, quantified by CF. The  $K_D$  is expected to be positively correlated with RIP and the 2:1 phyllosilicate content. However, this is not the case (Table A.4). The  $K_D$  is strongly negatively correlated with K concentrations. As expected, the CF correlates most strongly to cation composition of pore water, and especially with K concentration. The TF correlates negatively with 2:1 phyllosilicate content and very strongly with exchangeable K content. This shows that the influence of K is predominant in these substrate-plant systems.

**Table A.4**

The Pearson correlation coefficients estimated by row-wise method between  $K_D$ , CF and TF based on pore water concentrations after growth and the substrate or plant mean values ( $N = 16$ ) after log-transformation, except for the pH. The RIP was measured on the substrates after plant growth. Significant correlations are in bold with \*\*\*  $p < 0.001$ ; \*\*  $p < 0.01$ ; \*  $p < 0.05$ .

	$K_D$	CF	TF
Substrate			
2:1 minerals	<b>-0.58*</b>	<b>-0.75***</b>	<b>-0.55*</b>
RIP	0.28	-0.11	<b>-0.51*</b>
CEC	-0.04	-0.29	-0.43
pH	<b>-0.60*</b>	-0.48	-0.09
Exchangeable			
$^{137}\text{Cs}$	0.26	0.25	0.10
K (cohext)	<b>-0.66**</b>	<b>-0.94***</b>	<b>-0.75***</b>
K ( $\text{NH}_4\text{OAc}$ )	<b>-0.63**</b>	<b>-0.92***</b>	<b>-0.76***</b>
Pore water before			
$^{137}\text{Cs}$	<b>-0.83***</b>	<b>-0.52*</b>	0.12
K	<b>-0.84***</b>	<b>-0.80***</b>	-0.32
Pore water after			
$^{137}\text{Cs}$	-	-	-0.11
K	<b>-0.86***</b>	<b>-0.93***</b>	<b>-0.51*</b>
Plant			
yield	0.28	0.10	-0.17
$^{137}\text{Cs}$	0.12	-	-
K	<b>-0.93***</b>	<b>-0.83***</b>	-0.27

## References

- Absalom, J.P., Young, S.D., Crout, N.M.J., Nisbet, A.F., Woodman, R.F.M., Smolders, E., Gillett, A.G., 1999. Predicting soil to plant transfer of radiocesium using soil characteristics. *Environ. Sci. Technol.* 33, 1218–1223. <https://doi.org/10.1021/es9808853>.
- Absalom, J.P., Young, S.D., Crout, N.M.J., Sanchez, A., Wright, S.M., Smolders, E., Nisbet, A.F., Gillett, A.G., 2001. Predicting the transfer of radiocaesium from organic soils to plants using soil characteristics. *J. Environ. Radioact.* 52, 31–43. [https://doi.org/10.1016/S0265-931X\(00\)00098-9](https://doi.org/10.1016/S0265-931X(00)00098-9).
- Almahayni, T., Beresford, N.A., Crout, N.M.J., Sweeck, L., 2019. Fit-for-purpose modelling of radiocaesium soil-to-plant transfer for nuclear emergencies: a review. *J. Environ. Radioact.* 201, 58–66. <https://doi.org/10.1016/j.jenvrad.2019.01.006>.
- Bassett, W., 1960. Role of hydroxyl orientation in mica alteration. *Geol. Soc. Am.* 71, 449–456. [https://doi.org/10.1130/0016-7606\(1960\)71\[449:ROHOIM\]2.0.CO;2](https://doi.org/10.1130/0016-7606(1960)71[449:ROHOIM]2.0.CO;2).
- Bellenger, J.P., Staunton, S., 2008. Adsorption and desorption of  $85\text{Sr}$  and  $137\text{Cs}$  on reference minerals, with and without inorganic and organic surface coatings. *J. Environ. Radioact.* 99, 831–840. <https://doi.org/10.1016/j.jenvrad.2007.10.010>.
- Bunzl, K., Schimmmack, W., Krouglov, S.V., Alexakhin, R.M., 1995. Changes with time in the migration of radiocesium in the soil, as observed near Chernobyl and in Germany, 1986–1994. *Sci. Total Environ.* 175, 49–56. [https://doi.org/10.1016/0048-9697\(95\)04842-1](https://doi.org/10.1016/0048-9697(95)04842-1).
- Ciesielski, H., Sterckeman, T., 1997. Determination of cation exchange capacity and exchangeable cations in soils by means of cobalt hexamine trichlorideEffects of experimental conditions. *Agronomie* 17, 1–7. <https://doi.org/10.1051/agro:19970101>.
- Craen, M.De, Geet, M.Van, Honty, M., Weetjens, E., Sillen, X., 2008. Extent of oxidation in boom clay as a result of excavation and ventilation of the HADES URF: experimental and modelling assessments. *Phys. Chem. Earth* 33, S350–S362. <https://doi.org/10.1016/j.pce.2008.10.032>.
- Cremers, A., Elsens, A., De Preter, P., Maes, A., 1988. Quantitative analysis of radiocaesium retention in soils. *Nature* 335, 247–249. <https://doi.org/10.1038/335247a0>.
- D'Souza, T.J., Fagniart, E., Kirchmann, R., 1980. Effects of Clay Mineral Type and Organic Matter on the Uptake of Radiocesium by Pasture Plants. (BLG—538). Belgium.
- Desmet, G.M., Van Loon, L.R., Howard, B.J., 1991. Chemical speciation and bioavailability of elements in the environment and their relevance to radioecology. *Sci. Total Environ.* 100, 105–124. [https://doi.org/10.1016/0048-9697\(91\)90375-O](https://doi.org/10.1016/0048-9697(91)90375-O).
- Durrant, C.B., Begg, J.D., Kersting, A.B., Zavarin, M., 2018. Cesium sorption reversibility and kinetics on illite, montmorillonite, and kaolinite. *Sci. Total Environ.* 610–611, 511–520. <https://doi.org/10.1016/j.scitotenv.2017.08.122>.
- Eguchi, T., Ohta, T., Ishikawa, T., Matsunami, H., Takahashi, Y., Kubo, K., Yamaguchi, N., Kihou, N., Shinano, T., 2015. Influence of the nonexchangeable potassium of mica on radiocaesium uptake by paddy rice. *J. Environ. Radioact.* 147, 33–42. <https://doi.org/10.1016/j.jenvrad.2015.05.002>.
- Fanning, D.S., Keramidas, V.Z., El-Desoky, M.A., 1989. Micas. In: Dixon, J.B., Weed, S.B. (Eds.), Minerals in Soil Environments. SSSA Book Series <https://doi.org/10.2136/sssabookser1.2ed.c12>.
- Grim, R.E., 1968. *Clay Mineralogy*. second ed. McGraw-Hill, New York.
- Hoagland, D.R., Arnon, D.I., 1950. The water-culture method for growing plants without soil. *Circ. Calif. Agric. Exp. Stn.* 347, 32.
- International Atomic Energy Agency, 2009. Quantification of Radionuclide Transfer in Terrestrial and Freshwater Environments for Radiological Assessments. IAEA-TECDOC-1616. IAEA, Vienna.
- International Atomic Energy Agency, 2010. Handbook of Parameter Values for the Prediction of Radionuclide Transfer in Terrestrial and Freshwater Environments. Technical Reports Series No. 472. IAEA, Vienna.
- Jackson, M.L., 1975. *Soil Chemical Analysis: Advanced Course*. second. ed. Published by the author, Winsconsin.
- de Koning, A., 2007. Measuring the Specific Caesium Sorption Capacity of Soils, Sediments and Clay Minerals. 22, pp. 219–229. <https://doi.org/10.1016/j.apgeochem.2006.07.013>.
- de Koning, A., Comans, R.N.J., 2004. Reversibility of radiocaesium sorption on illite. *Geochim. Cosmochim. Acta* 68, 2815–2823. <https://doi.org/10.1016/j.gca.2003.12.025>.
- Missana, T., García-Gutiérrez, M., Benedicto, A., Ayora, C., De-Pourcq, K., 2014. Modelling of Cs sorption in natural mixed-clays and the effects of ion competition. *Appl. Geochem.* 49, 95–102. <https://doi.org/10.1016/j.apgeochem.2014.06.011>.
- Moore, D.M., Reynolds, R.C.J., 1997. *X-ray Diffraction and the Identification and Analysis of Clay Minerals*. second ed. Oxford University Press.
- Ogasawara, S., Nakao, A., Yanai, J., 2013. Radiocesium interception potential (RIP) of smectite and kaolin reference minerals containing illite (micaceous mineral) as impurity. *Soil Sci. Plant Nutr.* 59, 852–857. <https://doi.org/10.1080/00380768.2013.862158>.
- Sanchez, A.L., Wright, S.M., Smolders, E., Naylor, C., Stevens, P.A., Kennedy, V.H., Dodd, B.A., Singleton, D.L., Barnett, C.L., 1999. High plant uptake of radiocaesium from organic soils due to Cs mobility and low soil K content. *Environ. Sci. Technol.* 33, 2752–2757. <https://doi.org/10.1021/es990058h>.
- Sawhney, B.L., 1972. Selective sorption and fixation of cations by clay minerals: a review. *Clay Clay Miner.* 20, 93–100. <https://doi.org/10.1346/CCMN.1972.0200208>.
- Seple, K.T., Doick, K.J., Jones, K.C., Burwell, P., Craven, A., Harms, H., 2004. Defining bioavailability and bioaccessibility of contaminated soil and sediment is complicated. *Environ. Sci. Technol.* 38, 228A–231A. <https://doi.org/10.1021/es040548w>.
- Shaw, G., Bell, J.N.B., 1991. Competitive effects of potassium and ammonium on caesium uptake kinetics in wheat. *J. Environ. Radioact.* 13, 283–296. [https://doi.org/10.1016/0265-931X\(91\)90002-W](https://doi.org/10.1016/0265-931X(91)90002-W).
- Smolders, E., Van Den Brande, K., Merckx, R., 1997. Concentrations of  $^{137}\text{Cs}$  and K in soil solution plant availability of  $^{137}\text{Cs}$  in soils. *Environ. Sci. Technol.* 31, 3432–3438. <https://doi.org/10.1021/es970113r>.
- Środoń, J., Drits, V.A., McCarty, D.K., Hsieh, J.C.C., Eberl, D.D., 2001. Quantitative x-ray diffraction analysis of clay-bearing rocks from random preparations. *Clay Clay Miner.* 49, 514–528. <https://doi.org/10.1346/CCMN.2001.0490604>.
- Steiner, A.A., 1961. A universal method for preparing nutrient solutions of a certain desired composition. *Plant Soil* 15, 134–154. <https://doi.org/10.1007/BF01347224>.
- Tarsitano, D., Young, S.D., Crout, N.M.J., 2011. Evaluating and reducing a model of radiocaesium soil-plant uptake. *J. Environ. Radioact.* 102, 262–269. <https://doi.org/10.1016/j.jenvrad.2010.11.017>.
- Thiry, Y., 1997. Etude du cycle de radiocesium en écosystème forestier: Distribution et fractures de mobilité. Université Catholique de Louvain.
- Thiry, Y., Vandecasteele, C.M., Delvaux, B., 1996. Ability of Specimen Minerals to Fix Radiocaesium: Effect of the Chemical Environment. SCKCEN, Mol Belgium.
- Uematsu, S., Vandenhove, H., Sweeck, L., Van Hees, M., Wannijn, J., Smolders, E., 2016. Variability of the soil-to-plant radiocaesium transfer factor for Japanese soils predicted with soil and plant properties. *J. Environ. Radioact.* 153, 51–60. <https://doi.org/10.1016/j.jenvrad.2015.12.012>.
- USDA, 1954. Diagnosis and Improvement of Saline and Alkali Soils. Soil Science Society of America Journal. United States Department of Agriculture. Soil and Water Conservation Research Branch, Agricultural Research Service <https://doi.org/10.2136/sssaj1954.03615995001800030032x>.
- Wauters, J., Elsens, A., Cremers, A., Konoplev, A.V., Bulgakov, A.A., Comans, R.N.J., 1996a. Prediction of solid/liquid distribution coefficients of radiocaesium in soils and sediments.

- Part one: a simplified procedure for the solid phase characterisation. Appl. Geochem. 11, 589–594. [https://doi.org/10.1016/0883-2927\(96\)00027-3](https://doi.org/10.1016/0883-2927(96)00027-3).
- Wauters, J., Vidal, M., Elsen, A., Cremers, A., 1996b. Prediction of solid/liquid distribution coefficients of radiocaesium in soils and sediments. Part two: a new procedure for solid phase speciation of radiocaesium. Appl. Geochem. 11, 595–599. [https://doi.org/10.1016/0883-2927\(96\)00028-5](https://doi.org/10.1016/0883-2927(96)00028-5).
- Wauters, J., Elsen, A., Cremers, A., 1996c. Prediction of solid/liquid distribution coefficients of radiocaesium in soils and sediments. Part three: a quantitative test of a K (D) predictive equation. Appl. Geochem. 11, 601–603. [https://doi.org/10.1016/0883-2927\(96\)00029-7](https://doi.org/10.1016/0883-2927(96)00029-7).
- Zeelmaekers, E., 2011. In: Leuven, K.U. (Ed.), Computerized Qualitative and Quantitative Clay Mineralogy: Introduction and Application to Known Geological Cases. Faculteit Wetenschappen, Leuven ISBN: 978-90-8649-414-9.